ISSN 1674-1056
http://cpb.iphy.ac.cn
http://iopscience.iop.org/cpb
中国物理 B
Chinese Physics
中国物理
Chinese Physics B

Single SH guided wave mode generation method for PPM EMATs

Guo-Fu Zhai(翟国富), Yong-Qian Li(李永虔)
Citation: Chin. Phys. B . 2020, 29(5): 054303 . **doi:** 10.1088/1674-1056/ab81f8
Journal homepage: http://cpb.iphy.ac.cn; http://iopscience.iop.org/cpb

What follows is a list of articles you may be interested in

Lamb wave signal selective enhancement by an improved design of meander-coil electromagnetic acoustic transducer

Wen-Xiu Sun(孙文秀), Guo-Qiang Liu(刘国强), Hui Xia(夏慧), Zheng-Wu Xia(夏正武)
Chin. Phys. B . 2018, 27(8): 084301 . **doi:** 10.1088/1674-1056/27/8/084301

Selective generation of ultrasonic Lamb waves by electromagnetic acoustic transducers

Ming-Liang Li(李明亮), Ming-Xi Deng(邓明晰), Guang-Jian Gao(高广健)
Chin. Phys. B . 2016, 25(12): 124301 . **doi:** 10.1088/1674-1056/25/12/124301

Relationships of the internodal distance of biological tissue with its sound velocity and attenuation at high frequency in doublet mechanics

Cheng Kai-Xuan, Wu Rong-Rong, Liu Xiao-Zhou, Liu Jie-Hui, Gong Xiu-Fen, Wu Jun-Ru
Chin. Phys. B . 2015, 24(4): 044302 . **doi:** 10.1088/1674-1056/24/4/044302

Axisymmetric wave propagation in gas shear flow confined by a rigid-walled pipeline

Chen Yong, Huang Yi-Yong, Chen Xiao-Qian, Bai Yu-Zhu, Tan Xiao-Dong
Chin. Phys. B . 2015, 24(4): 044301 . **doi:** 10.1088/1674-1056/24/4/044301

Study of acoustic bubble cluster dynamics using a lattice Boltzmann model

Mahdi Daemi, Mohammad Taeibi-Rahni, Hamidreza Massah
Chin. Phys. B . 2015, 24(2): 024302 . **doi:** 10.1088/1674-1056/24/2/024302

Single SH guided wave mode generation method for PPM EMATs*

Guo-Fu Zhai(翟国富) and Yong-Qian Li(李永虔)†

Institute of Reliability in Electrical Apparatus and Electronics, Harbin Institute of Technology, Harbin 150001, *China*

(Received 6 December 2019; revised manuscript received 12 March 2020; accepted manuscript online 23 March 2020)

Using periodic permanent magnet (PPM) electromagnetic acoustic transducers (EMATs), different shear horizontal (SH) guided wave modes can form simultaneously in some situations, which can interfere with the inspection. The main cause of this phenomenon (typically named multiple modes) is related to the frequency bandwidth of excitation signals and the transducer spatial bandwidth. Simply narrowing the frequency bandwidth cannot effectively limit the number of different SH modes. Previous researches showed that unnecessary SH wave modes can be eliminated by using dual EMATs. However, in practical applications, it is more convenient to change the excitation frequency than to use dual EMATs. In this paper, the stress boundary conditions of the PPM-EMAT are analyzed, the analytical expression of SH guided wave is established, and the magnitude of SH guided wave mode under continuous tone and tone-burst input is obtained. A method to generate a single SH mode by re-selecting an operating point is proposed. Furthermore, the influence of the frequency bandwidth of the tone-burst signal is analyzed. Finally, a single SH mode excitation is achieved with tone-burst input.

Keywords: operating point, multiple modes, SH guided waves, electromagnetic acoustic transducer (EMAT)

PACS: 43.38.Dv, 43.20.Ks, 43.35.Cg **DOI:** 10.1088/1674-1056/ab81f8

1. Introduction

Ultrasonic guided waves have been widely studied and applied to nondestructive testing because of their low attenuation and large volume coverage. Shear horizontal (SH) guided waves have simple dispersion characteristics. Being nondispersive and having the particle motion in the plane of the plate, the SH0 mode is sensitive to defects that are either perpendicular or parallel to the wave vector.[1–3] These good characteristics enable SH guided waves to be applied to increasing applications such as crack detection,[2–4] corrosion detection,[5,6] weld detection,[7–9] and the evaluation of interfacial adhesion.[10]

SH guided waves can be generated by piezoelectric transducers, but piezoelectric transducers need to be specially designed and attached to plates by a very viscous or solid couplant,[11] making it difficult to apply to online detection. Therefore, SH guided waves are commonly generated by electromagnetic acoustic transducers (EMATs) which are simple in structure and need no couplant.[12]

According to the dispersion characteristics of SH guided waves, the frequency-thickness product is negatively correlated with the wavelength-thickness ratio. If the frequency-thickness product is very low or the wavelength-thickness ratio is very large, only the SH0 mode can be generated. However, in some applications, there are the cases of high frequency-thickness product or low wavelength-thickness ratio, such as (i) high frequency in order to improve accuracy;[13] (ii) the thickness of samples is large but the wavelength of SH guided waves generated by EMATs cannot be too large.[14] Once the excitation frequency exceeds the cut-off frequency of a certain mode, multiple modes occur.[15] The appearance of the multi-mode phenomenon will lead to some adverse phenomena: i) the superposition of multiple modes will weaken the vibration at some positions, where defects may not be able to be detected;[15] ii) multiple SH modes will be superimposed when the detection range is small. The waveform is difficult to analyze in this circumstance.

The multi-modes phenomenon is caused by the frequency bandwidth of exciting signals and the transducer spatial bandwidth.[16] Simply narrowing the frequency bandwidth of exciting signals cannot effectively reduce the production of multiple modes, meaning that the influence of transducer spatial bandwidth cannot be neglected, because the continuous sine tone (namely, a single frequency) can still excite multiple modes of SH guided waves.[15] However, in previous studies, the effect of spatial bandwidth on multi-modes was not evident.

A single and pure SH guided wave mode can be effectively generated by dual EMATs.[17,18] However, the dual EMATs cannot work well in practice and there are few other efficient ways to generate a single SH mode.

According to the expression of SH modes' amplitude coefficients, which relates to the excitation frequency and the EMAT's geometrical parameters, in this paper we study the method of suppressing unwanted modes by selecting an appropriate operating point and the frequency bandwidth of the excitation signal. Theoretical analyses and experimental re-

*Project supported by the National Natural Science Foundation of China (Grant No. 51977044).

†Corresponding author. E-mail: 15B906029@hit.edu.cn

© 2020 Chinese Physical Society and IOP Publishing Ltd

sults prove that a single SH mode can be obtained.

2. Theoretical fundamentals

2.1. Boundary conditions

SH guided waves are usually generated and detected by EMATs chiefly via two kinds of physical mechanisms: the Lorentz force mechanism when the material is conductive and the magnetostriction mechanism when the material is ferromagnetic.[12] Only the Lorentz force mechanism is considered in this paper.

Periodic permanent magnet (PPM) EMATs are generally used to generate SH guided waves. The structure of a PPM EMAT is shown in Fig. 1. A PPM EMAT consists of a racetrack coil and a magnet array that provides static magnetic fields perpendicular to the plate.

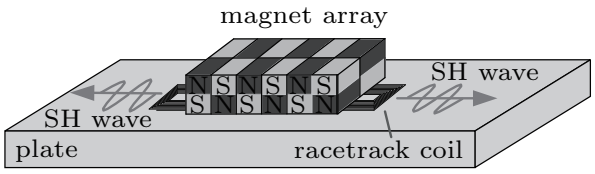


Fig. 1. Structure of a PPM EMAT on a plate.

Figure 2 shows the distribution of the Lorentz force. The parameter d is the thickness of the plate, l is the width of each magnet, and L is the spatial period of the magnet array, which is twice as large as the center spacing of adjacent magnets. In general, L is equal to the wavelength of SH guide waves.[16]

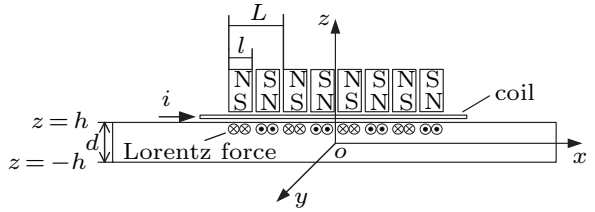


Fig. 2. Distribution of Lorentz force.

For the SH modes, the particle displacement vectors have only a y component. That is, the particle displacement in the x direction is zero, and so is it in the z direction. The particle displacement in the y direction is $u_y(x,z)$.[1] The traction component τ_{zy} is given by[1]

$$\tau_{zy} = \mu \frac{\partial u_y}{\partial z},$$

where μ is the shear modulus of the specimen.

Since the skin depth of eddy current is far less than the acoustic wavelength at the same frequency and the thickness of sample, the Lorentz force distributed in the skin depth can approximately be regarded as the surface stress at $z = h$ ($h = d/2$).[19–21] Due to the surface stress, the upper surface of the plate is not a free boundary, while the lower surface is still a free one. Assuming that the distribution function of the upper surface stress is $g(x)$, the boundary conditions at the upper and lower surfaces of the plate are

$$\tau_{zy}(x, z = h) = g(x), \tag{1}$$

$$\tau_{zy}(x, z = -h) = 0. \tag{2}$$

The upper surface stress $g(x)$ is as follows:

$$g(x) = J(x) \times B(x),$$

where $J(x)$ is the eddy-current distribution and $B(x)$ is the magnetic-field distribution.

In the classical Lorentz force model of EMATs, within the transducer area the magnetic field and the eddy current are thought to be constant and uniformly distributed.[11,19–21] And outside the transducer area, the magnetic field and the eddy current are thought to be zero. Therefore, the distribution function $g(x)$ can approximately be regarded as a function shown in Fig. 3. The amplitude of the function is assumed to be A_g. In fact, when the finite element method is applied to the solid mechanics simulation, the distribution function of the stress usually used by researchers is consistent with the function shown in Fig. 3.[15,22]

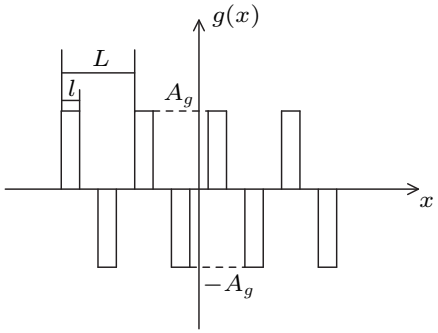


Fig. 3. Distribution function of surface stress.

2.2. Analytical expression with continuous tone input

In Ref. [1], the stress boundary conditions of piezoelectric transducers are

$$\tau_{zy}(x, z = h) = \cos(\theta) g(x) \exp(\mathrm{i} k_w \sin(\theta) x),$$

$$\tau_{zy}(x, z = -h) = 0,$$

where θ is the incident angle of the wedge of the piezoelectric transducer with respect to the normal to the surface of the layer and k_{w} represents the shear wavenumber in the wedge.

The displacement equation of SH guided wave is

$$u_y = \sum_{n=0,2,4,\cdots}^{\infty} A_n u_{yn}^{\mathrm{s}} + \sum_{n=1,3,5,\ldots}^{\infty} B_n u_{yn}^{\mathrm{a}}, \tag{3}$$

$$u_{yn}^{\mathrm{s}} = \cos(q_n z) \exp[\mathrm{i}(k_n x - \omega t)],$$

$$u_{yn}^{\mathrm{a}} = \sin(q_n z) \exp[\mathrm{i}(k_n x - \omega t)], \tag{4}$$

$$\omega = 2\pi f,$$

$$q_n = \frac{n\pi}{2h},$$

$$k_n = \sqrt{\left(\frac{\omega}{c_s}\right)^2 - \left(\frac{n\pi}{2h}\right)^2},$$

where u_y is the total displacement, u_{yn}^{s} is the displacement of the n-th symmetric mode, u_{yn}^{a} is the displacement of the n-th antisymmetric mode, ω is the angular frequency, and k_n is the wavenumber of the n-th SH guided wave mode, f is the frequency of SH guided wave, c_s is the velocity of the shear wave, and A_0, A_n, and B_n are called amplitude coefficients. When SH guided wave is generated by piezoelectric transducer, amplitude coefficients are[1]

$$\begin{aligned} A_0 &= \frac{\mathrm{i}}{4\mu h k_0}\cos(\theta)\hat{g}(k_0 - k_w\sin(\theta)), \\ A_n &= \frac{(-1)^{n/2}\mathrm{i}}{2\mu h k_n}\cos(\theta)\hat{g}(k_n - k_w\sin(\theta)) \\ &\quad (n \in (2,4,6,\ldots)), \\ B_n &= \frac{(-1)^{(n-1)/2}\mathrm{i}}{2\mu h k_n}\cos(\theta)\hat{g}(k_n - k_w\sin(\theta)) \\ &\quad (n \in (1,3,5,\ldots)), \end{aligned}$$

where $\hat{g}(x)$ is the Fourier transform of $g(x)$.

Comparing Eqs. (1) and (2), and the stress boundary conditions of piezoelectric transducers, it can be found that the PPM-EMAT can be regarded as a piezoelectric transducer with an incident angle of zero.[1] Therefore, the amplitude coefficients of SH guided wave generated by PPM EMAT can be obtained as follows:

$$A_0 = \frac{\mathrm{i}}{4\mu h k_0}\hat{g}(k_0), \tag{5}$$

$$A_n = \frac{(-1)^{n/2}\mathrm{i}}{2\mu h k_n}\hat{g}(k_n) \quad (n \in (2,4,6,\ldots)), \tag{6}$$

$$B_n = \frac{(-1)^{(n-1)/2}\mathrm{i}}{2\mu h k_n}\hat{g}(k_n) \quad (n \in (1,3,5,\ldots)). \tag{7}$$

The magnitudes of the amplitude coefficients are

$$\Phi_n = \frac{1}{\varepsilon_n \mu\sqrt{(fd/c_s)^2 - (n/2)^2}}\left|\hat{g}\left(\frac{2\pi}{\lambda}\right)\right|, \tag{8}$$

where $\varepsilon_0 = 4\pi, \varepsilon_n = 2\pi$, and λ is the wavelength of SH guided wave.

The dispersion equation of SH guided wave is

$$\left(\frac{fd}{c_s}\right)^2 - \frac{1}{(\lambda/d)^2} = \frac{n^2}{4}. \tag{9}$$

Then equation (8) can be expressed as

$$\Phi_n = \frac{1}{\varepsilon_n \mu\sqrt{(fd/c_s)^2 - (n/2)^2}}\left|\hat{g}\left(\frac{2\pi}{\sqrt{(f/c_s)^2 - (n/2d)^2}}\right)\right|. \tag{10}$$

Equation (8) can also be expressed as

$$\Phi_n = \frac{\lambda/d}{\varepsilon_n \mu}\left|\hat{g}\left(\frac{2\pi}{\lambda}\right)\right|. \tag{11}$$

It can be concluded from Eq. (11) that the magnitude of each SH wave mode is inversely proportional to the thickness of the plate. The magnitude of the SH0 mode is the smallest in fixed thickness, while other modes have the same magnitude that is twice as large as the magnitude of the SH0 mode.

Equation (10) can be divided into two components

$$\Gamma_n = \frac{1}{\varepsilon_n \mu\sqrt{(fd/c_s)^2 - (n/2)^2}} = \frac{\lambda/d}{\varepsilon_n \mu}, \tag{12}$$

$$\Psi_n = \left|\hat{g}\left(\frac{2\pi}{\sqrt{(f/c_s)^2 - (n/2d)^2}}\right)\right| = \left|\hat{g}\left(\frac{2\pi}{\lambda}\right)\right|, \tag{13}$$

where Γ_n component is independent of the profile of transducer, which is called the excitation function in Ref. [1] and Ψ_n is the magnitude of $\hat{g}(x)$, which is called the transducer spatial function in this paper. The value of this component is related to parameters of the PPM EMAT.

2.3. Magnitude with tone-burst input

The analytical expression of SH guided wave described above is based on a single frequency signal expressed as a single frequency continuous sine tone in practice. However, in practical applications, transient excitation signals are generally used and the commonly used transient excitation signal is the tone-burst signal.

Assuming that the function of the tone-burst signal is $f(t)$ and its Fourier transform is $F(\omega)$. The magnitude of the amplitude coefficients is

$$\Phi_{nw} = \frac{1}{\varepsilon_n \mu\sqrt{(fd/c_s)^2 - (n/2)^2}}\left|\hat{g}\left(\frac{2\pi}{\lambda}\right)\right|F(\omega). \tag{14}$$

In practical applications, the parameters of detecting transducer are always the same as those of transmitting transducer. By taking this into account, the magnitude of the amplitude coefficient of each SH guided wave mode received by the detecting transducer is

$$\Phi_{nwr} = \frac{1}{\varepsilon_n \mu\sqrt{(fd/c_s)^2 - (n/2)^2}}\left|\hat{g}\left(\frac{2\pi}{\lambda}\right)\right|^2 F(\omega). \tag{15}$$

In this paper, to make the distinction, Φ_n is referred to as the single-frequency magnitude, Φ_{nw} as the transient magnitude, and Φ_{nwr} as the received magnitude.

3. Method of suppressing unwanted modes

It can be concluded from Eqs. (10), (14), and (15) that the magnitude of each SH guided wave mode is related to not only the excitation frequency, but also the parameters of transducer and the thickness of plate. These parameters are appointed to introduce the method of suppressing unwanted SH guided wave mode. The transducer parameters and plate thickness

shown in Table 1 are selected. The design objective is to obtain a single SH0 mode and suppress other SH modes in this paper.

Table 1. Parameters of PPM-EMAT and plate used in this paper.

Parameter	Value
l/mm	3
L/mm	6
d/mm	5
Number of magnets	6
Material of plate	aluminum
Velocity of shear wave	3114 m/s

3.1. Operating point selection

In general, the operating point is chosen according to Eq. (9). The spatial period of the magnet array is 6 mm, so the wavelength of SH guided waves is 6 mm. The excitation frequency is chosen as 0.52 MHz according to Eq. (9). The cut-off frequency of the SH1 mode is about 0.311 MHz, and the cut-off frequency of the SH2 mode is about 0.623 MHz. So, the SH0 mode and SH1 mode can be generated under the given parameters of the EMAT. Taking the numerical solutions of Eq. (10), the single-frequency magnitude curve of the SH0 mode and SH1 mode are shown in Fig. 4. Currently, the normalized single-frequency magnitude of the SH0 mode is 0.36, and the normalized single-frequency magnitude of the SH1 mode is 0.56. Then, the total displacement of each position in the plate can be calculated by Eqs. (3) and (4). And the maximum displacement of each position is recorded. The plots that are shown in Fig. 5(a) represent the maximum displacement at each point in the plate. Each maximum displacement is normalized to a range from zero to one. The horizontal axis represents the distance from the transducer. A series of fringes is observed in Fig. 5(a), and the maximum displacements of some positions are almost zero. The reason for this phenomenon is that both the SH0 and SH1 modes exist simultaneously in the plate, and it is the result of displacement superposition of the two modes.

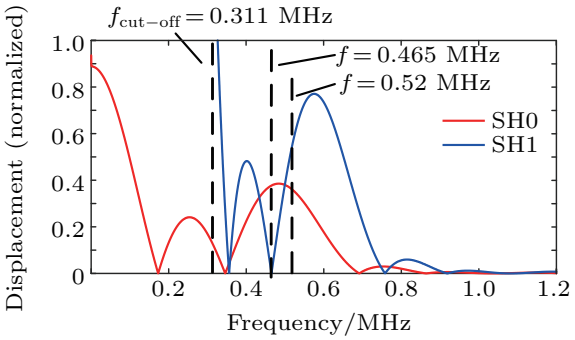


Fig. 4. Single-frequency magnitude curves of SH guided wave modes.

It can be seen from Fig. 4 that the single-frequency magnitudes of both modes can be controlled by adjusting the excitation frequency. When the excitation frequency is adjusted to 0.465 MHz, the single-frequency magnitude of the SH1 mode is almost zero. Therefore, if the excitation frequency is chosen to be 0.465 MHz, only the SH0 mode can be generated theoretically, and no SH1 mode can be generated. Then the unwanted SH1 mode can be effectively suppressed.

Therefore, the excitation frequency is changed into 0.465 MHz. It is calculated that the single-frequency magnitude of the SH1 mode is only 2.8% of that of the SH0 mode. Similarly, the maximum displacement of each position in the plate is calculated, and the normalized maximum displacement at each point is shown in Fig. 5(b). The minimum value in the plot is 0.97, which is approximately equal to the maximum value, demonstrating that the SH1 mode is effectively suppressed, and the SH0 mode is the absolute main component of the guided wave.

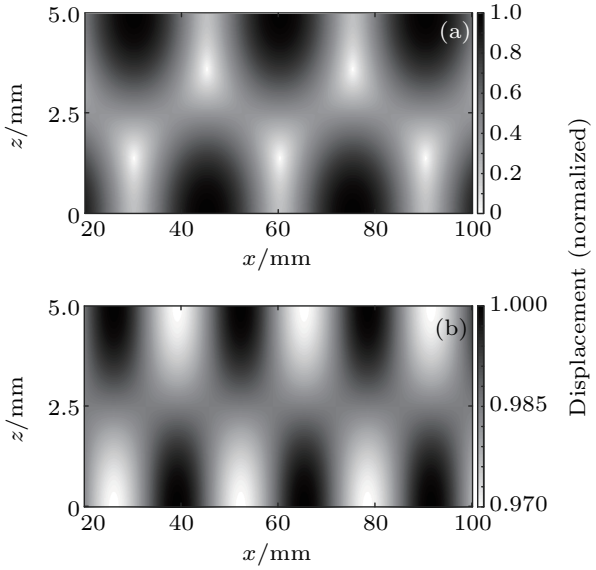


Fig. 5. Normalized maximum displacement at each point in plate at input frequency of (a) 0.52 MHz and (b) 0.465 MHz.

3.2. Influence of frequency bandwidth with tone-burst input

In practice, the excitation signal is always the tone-burst signal. When the transient excitation signal is an eight-cycle sinusoidal signal with a center frequency of 0.465 MHz modulated by the Hanning window, the received magnitude curves of SH modes are shown in Fig. 6(b) by solving Eq. (15). The excitation signal is shown in Fig. 6(a).

It can be seen from Fig. 6 that the SH guided waves received by a detecting transducer includes an SH0 mode with a center frequency of 0.476 MHz, an SH1 mode with a center frequency of 0.525 MHz and an SH1 mode with a center frequency of 0.418 MHz. So, there are two SH1 modes received by the detecting transducer, which are represented by two wave packets on the time domain waveform (see Fig. 10 in Section 4). Next, the rest of this subsection focuses on explaining why two SH1 modes are generated.

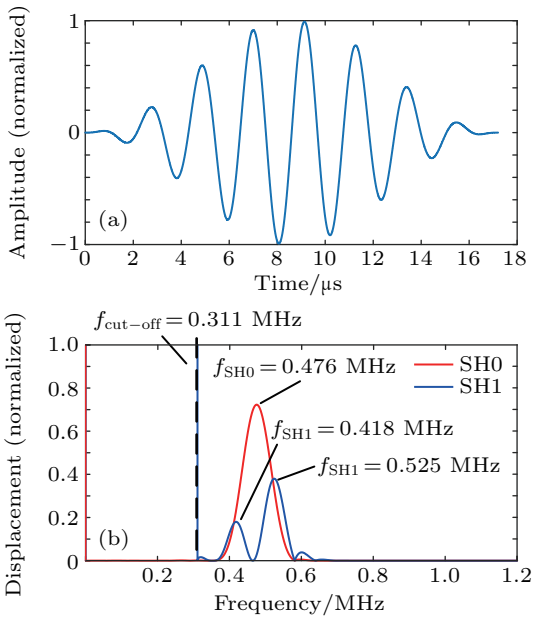


Fig. 6. (a) Transient excitation signal and (b) received magnitude curves of SH guided wave modes.

The relationship between the excitation function and the frequency-thickness product obtained by solving Eq. (12) and shown in Fig. 7(a) (this figure can be seen in Ref. [1]). For each SH wave mode, the larger frequency-thickness product reduces the magnitude of the SH guided wave. For the same frequency-thickness product, the higher-order wave mode has a larger magnitude.

The relationship between the transducer spatial function and frequency-thickness product is obtained by solving Eq. (13) and shown in Fig. 7(b). It demonstrates that for the same transducer, the maximum transducer spatial function magnitude of each mode is the same.

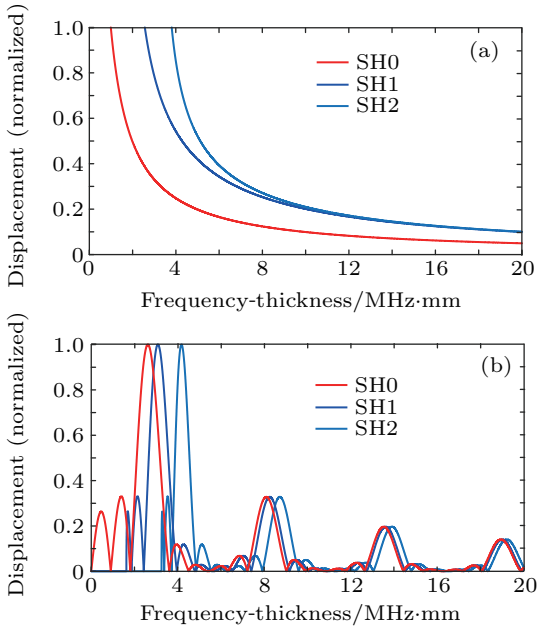


Fig. 7. Displacements *versus* frequency-thickness for (a) excitation function and (b) transducer spatial function.

It can be seen from Fig. 7(b) that no matter which SH guided wave mode it belongs to, the transducer spatial function curve of this mode contains a main lobe and some side lobes. Taking the SH1 mode for example, the excitation function, the transducer spatial function, and the single-frequency magnitude of the SH1 mode are plotted in Fig. 8. The transducer spatial function magnitude of the left-side lobe is higher than that of the right-side lobe. In addition, the excitation function magnitude at low frequency is greater than that at high frequency. As a result, the single-frequency magnitude of SH guided wave generated by the right-side lobes is so small that it can be ignored. However, the single-frequency magnitude of SH guided wave generated by the left-side lobe is large, sometimes even close to that generated by the main lobe. Therefore, When the frequency bandwidth of the excitation signal is wide, the received magnitude of SH guided waves generated by the left-side lobes and by the main lobe are close, which will result in the co-existence of two SH1 modes with different center frequencies. The SH1 mode example is investigated as done above, but the conclusion above is applicable to other modes as well.

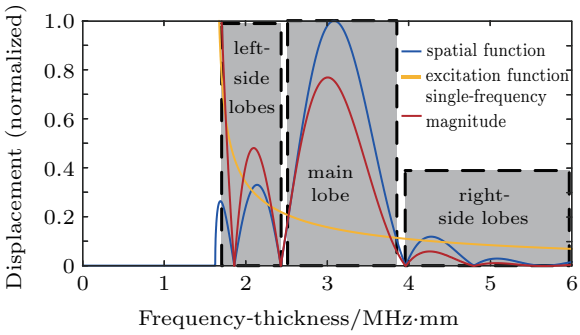


Fig. 8. Displacements *versus* frequency-thickness for tranducer spatial function, excitation function, and the single-frequency magnitude of SH1 mode.

3.3. Mode suppression with tone-burst input

The reason that two SH1 modes are generated at the same time is that the excitation signal has a wide frequency bandwidth. Therefore, reducing the frequency bandwidth of the excitation signal is an effective way to implement the mode suppression. As can be seen from Fig. 6, when the frequency bandwidth of the excitation signal is narrower than 0.465 MHz ±0.05 MHz, the two SH1 modes can be effectively suppressed.

The new excitation signal is a 25-cycle sinusoidal tone with a center frequency of 0.465 MHz modulated by the Hanning window. The frequency bandwidth of the new excitation signal is about 0.465 MHz ± 0.04 MHz. At this time, the relationship between the received magnitude and frequency is shown in Fig. 9. The maximum received magnitude of the SH1 mode is only 6% of that of the SH0 mode. The SH1 mode is greatly suppressed. Excitation signals with more cycles have narrower bandwidths, leading to a better result.

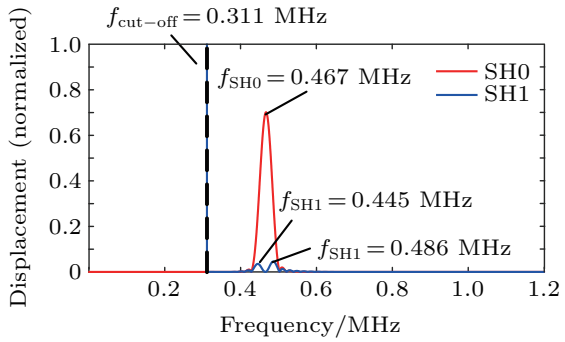


Fig. 9. Displacement–frequency curves of SH-guided wave modes when excitation signal has 25 cycles.

4. Experiment

Figure 10 shows the experiment platform used in this study. The parameters of the PPM EMAT and the plate used in the experiment are listed in Table 1. The PPM-EMAT was excited by Ritec RAM-5000 SNAP, which generated an eight-cycle sinusoidal tone with a center frequency of 0.465 MHz modulated by the Hanning window. The center distance between the generator and the detector was $s = 400$ mm.

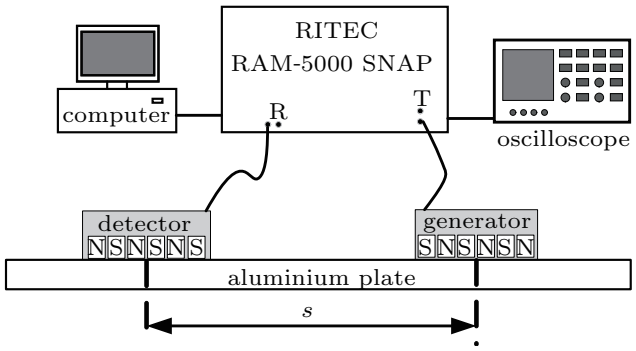


Fig. 10. Experiment platform.

According to the theoretical analysis, the received signal should include an SH0 mode with a central frequency of 0.476 MHz, an SH1 mode of 0.418 MHz, and an SH1 mode of 0.525 MHz. According to the dispersion curves of SH guided wave, the group velocities of the three wave modes were 3114 m/s, 2078 m/s, and 2507 m/s, respectively. The theoretical arrival times of the three wave modes were about 128 μs, 192 μs, and 159 μs, respectively.

The actually received signal and its short-time Fourier transform (STFT) spectrogram are shown in Fig. 11. It is worth noting that the main bang was not considered in Fig. 11(b). The function "spectrogram" performs the STFT in Matlab, and its input parameters were as follows: the data were the received signal data, whose length was 12000; the window was Hanning, whose length was 2048; the NFFT was 16384; the noverlap was 2047; the sampling rate was 32 Msps. The result showed that it mainly contained an SH0 mode of 0.477 MHz, an SH1 mode of 0.418 MHz, and an SH1 mode of 0.525 MHz, and the actual arrival times of the three wave modes were about 129 μs, 190 μs, and 153 μs, respectively. Considering the measurement error, the experimental results were in accordance with the theoretical analyses.

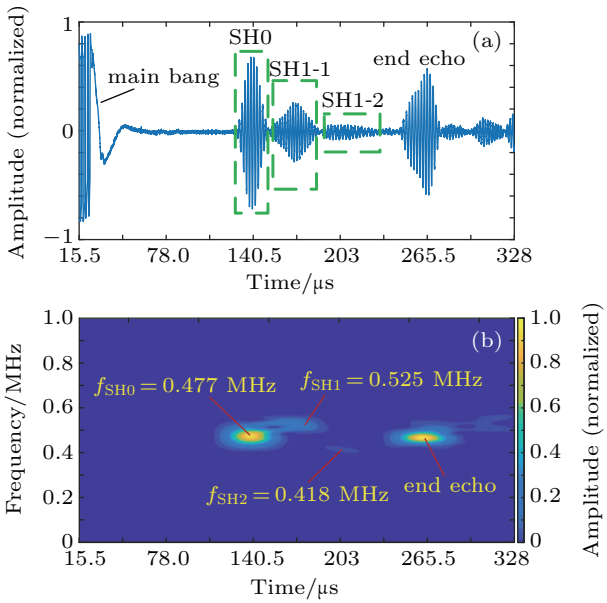


Fig. 11. (a) The receiving signal of the detector and (b) its STFT spectrogram when excitation signal has 8 cycles.

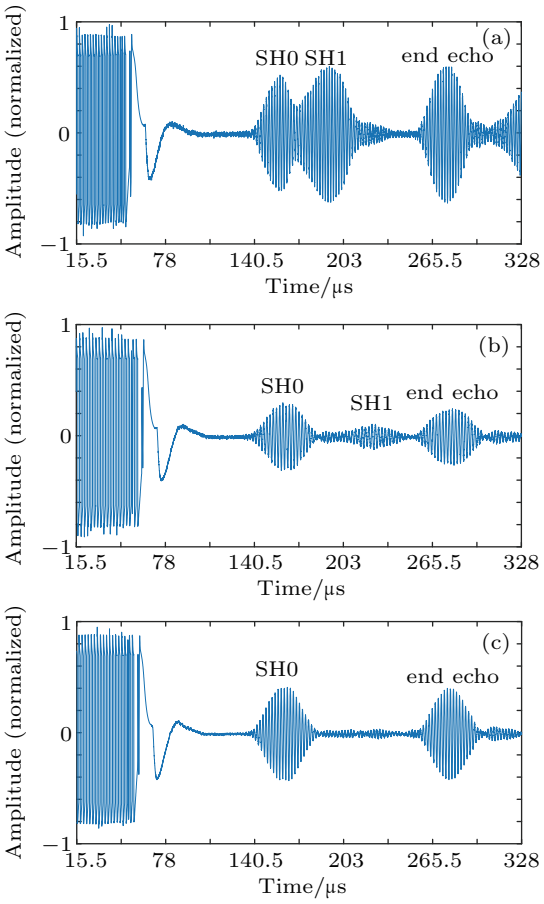


Fig. 12. Received signal of detector when excitation signal has 25 cycles at a frequency of (a) 0.52 MHz, (b) 0.44 MHz, (c) 0.465 MHz.

The cycle number of the excitation signal was modified to be 25. The frequencies of excitation signals were

0.52 MHz, 0.44 MHz, and 0.465 MHz. The resulting waveforms are shown in Fig. 12. The guided waves of 0.52 MHz and 0.44 MHz both included the SH1 mode, but the guided wave of 0.465 MHz had a small magnitude SH1 mode, which indicated that the SH1 mode was greatly suppressed. The experimental results agreed with the theoretical analyses.

The experimental results show that (I) both the main lobe and side lobes of the transducer spatial function can generate guided waves; (II) when the frequency bandwidth of the excitation signal is wide, the magnitude of SH guided wave generated by left-side lobes is large, which will aggravate the multi-mode phenomenon; (III) the unwanted SH modes cannot be suppressed at too high or too low a frequency and thus can be suppressed only by selecting an appropriate operating point and the frequency bandwidth of the excitation signal.

5. Conclusions

We have analyzed the stress boundary conditions of PPM-EMATs, established an analytical expression of SH guided wave generated by EMAT, and obtained the magnitude of SH guided wave modes under continuous tone and tone-burst input. It is proved that the magnitude of each SH mode is related to not only the excitation frequency, but also the parameters of the PPM EMATs and the thickness of plates. The analytical expression provides a theoretical basis for mode suppression.

Taking a specific transducer for example, in order to obtain a single SH0 mode and suppress other SH modes, the relationship between the single-frequency magnitude and frequency of each SH mode is investigated. If the excitation frequency of the SH0 mode is selected according to the traditional method, the SH1 mode is generated at the same time. However, by changing the operating point to a point where the magnitude of the SH1 mode is almost zero, the excitation of a single SH0 mode can be achieved.

The influence of the frequency bandwidth is analyzed here in this work. When the excitation signal is a tone-burst signal with a wide frequency bandwidth, in addition to the SH0 mode, there are also two SH1 modes with different center frequencies, because the SH guided waves generated by the left-side lobes and the main lobe coexist due to similar magnitude. This is a special phenomenon of SH guided wave.

Finally, the frequency bandwidth of the excitation signal is controlled. The two SH1 modes are effectively suppressed and the excitation of a single SH0 mode is achieved, which not only proves that the theoretical analysis is correct, but also confirms that a single SH guided wave mode can be generated by selecting an appropriate operating point and a frequency bandwidth of the excitation signal.

References

[1] Rose J L 1999 *Ultrasonic waves in solid media* (Cambridge: Cambridge University Press)
[2] Ratassepp M, Lowe J S, Cawley P and Klauson A 2008 *J. Acoust. Soc. Am.* **124** 2873
[3] Liang C, Kogia M, Mohimi A, Kappatos V, Selcuk C and Gan T H 2017 *Renew. Energy* **101** 771
[4] Ma Q Z, Jiao J P, Hu P, Zhong X, Wu B and He C F 2014 *Chin. J. Mech. Eng.* **27** 428
[5] Hirao M and Ogi H 1999 *NDT E Int.* **32** 127
[6] AndruschakN, Saletes I, Filleter T and Sinclair A 2015 *NDT E Int.* **75** 72
[7] Choi S, Cho H and Lissenden C J 2018 *Nucl. Eng. Technol.* **50** 890
[8] Lee J H and Kim D H 2014 *Int. J. Precis. Eng. Manuf.* **15** 2051
[9] Petcher P A and Dixon S 2015 *NDT E Int.* **74** 58
[10] Castaings M 2014 *Ultrasonics* **54** 1760
[11] Vasile C F and Thompson R B 1979 *J. Appl. Phys.* **50** 2583
[12] Ribichini R, Cegla F, Nagy P B and Cawley P 2011 *IEEE Trans. Ultrason. Ferroelectr. Freq. Control* **58** 2571
[13] Kwon Y, Kim H W and Kim Y Y 2015 *Ultrasonics* **62** 237
[14] Choi S, Cho H and Lissenden C J 2017 *Sensors* **17** 5
[15] Petcher P A and Dixon S 2017 *Nondestruct. Test. Eval.* **32** 113
[16] Dixon S, Petcher P A, Fan Y, Maisey D and Nickolds P 2013 *J. Phys. D-Appl. Phys.* **46** 445502
[17] Kubrusly A C, Freitas M A, Von Der Weid J P and Dixon S 2018 *IEEE Trans. Ultrason. Ferroelectr. Freq. Control* **65** 1239
[18] Qiu G Z, Song X C, Zhang X, Tu J and Chen T 2019 *Sensors* **19** 3019
[19] Li M L, Deng M X and Gao G J 2016 *Chin. Phys. B* **25** 124301
[20] Hirao M and Ogi H 2018 *Electromagnetic Acoustic Transducers: Noncontacting Ultrasonic Measurements using EMATs*, 2nd edn. (Japan: Springer) pp. 17–21
[21] Sun W X, Liu G Q, Xia H and Xia Z W 2018 *Chin. Phys. B* **27** 084301
[22] Advani S, Van Velsor J and Rose J L 2011 *6th IEEE Sensors Applications Symposium*, SAS, February 22–24, 2011, San Antonio, USA pp. 277–282